Am J Transl Res 2026;18(9):8109-8124
www.ajtr.org /ISSN:1943-8141/AJTR0174417

Original Article

Knockdown of circFNDC3B inhibits tumor growth and enhances cisplatin sensitivity in oral squamous cell carcinoma via the miR-206/ANXA2 axis

Jiahong Zhao[1*], Jie Guo[1*], Qi Sun[2], Zhihui Sun[3], Fei Xu[4], Yang Bai[4], Kunshan Li[1]

[1]Department of Stomatology, The Fourth Hospital of Hebei Medical University, Shijiazhuang 050000, Hebei, China; [2]Department of Stomatology, Hebei Children's Hospital, Shijiazhuang 050031, Hebei, China; [3]Department of Stomatology, Handan Central Hospital, Handan 056000, Hebei, China; [4]Department of Stomatology, Qinhuangdao Haigang Hospital, Qinhuangdao 066000, Hebei, China. [*]Equal contributors.

Received June 1, 2026; Accepted July 30, 2026; Epub September 15, 2026; Published September 30, 2026

Abstract: Background: Cisplatin (DDP)-based systemic chemotherapy is the standard first-line treatment for advanced oral squamous cell carcinoma (OSCC). However, its clinical utility is significantly limited by the high incidence of acquired drug resistance. In this study, we explored the biological function of circFNDC3B in regulating DDP resistance of OSCC and clarify its underlying molecular regulatory mechanism. Methods: The expression levels of circFNDC3B, miR-206 and ANXA2 in DDP-sensitive and DDP-resistant OSCC clinical tissues as well as corresponding cell lines were measured using qRT-PCR and western blotting. Dual-luciferase reporter experiments were performed to verify the direct binding relationship between miR-206 and circFNDC3B/Annexin A2 (ANXA2). A series of functional assays were further carried out to evaluate the effects of the circFNDC3B/miR-206/ANXA2 axis on the malignant phenotypes of drug-resistant OSCC cells. Besides, BALB/c nude mice xenograft models were established to assess the influence of circFNDC3B knockdown on tumorigenesis and DDP resistance in vivo. Results: circFNDC3B expression was markedly upregulated in DDP-resistant OSCC tumor samples. Silencing circFNDC3B significantly attenuated DDP resistance, suppressed the viability of DDP-resistant OSCC cells, and promoted apoptosis. Mechanistically, circFNDC3B directly targeted miR-206. The miR-206 inhibitor effectively eliminated the suppressive influence of circFNDC3B silencing on the malignant progression of DDP-resistant OSCC cells. Furthermore, miR-206 directly targeted ANXA2. Overexpression of ANXA2 via pcDNA-ANXA2 significantly counteracted the suppressive effects of miR-206 overexpression on the malignant progression of DDP-resistant OSCC cells. In vivo studies confirmed that knockdown of circFNDC3B substantially inhibited tumor growth. Conclusion: Knockdown of circFNDC3B inhibits tumor growth and enhances cisplatin sensitivity, thereby suppressing the malignant progression of OSCC cells via miR-206/ANXA2 axis.

Keywords: CircFNDC3B, oral squamous cell carcinoma, DDP resistance, miR-206, ANXA2

Introduction

Oral squamous cell carcinoma (OSCC) is a common malignancy of the head and neck region. Epidemiological studies indicate that OSCC is associated with high incidence and mortality rates. Owing to its anatomical location in the maxillofacial area, as well as its proximity to vital organs, treatment is challenging and often yields a poor prognosis, posing a substantial threat to human health [1]. Numerous etiological factors are involved in OSCC development, including tobacco use, alcohol consumption, betel nut chewing, nutritional deficiencies, inadequate oral hygiene, and viral infections [2]. Currently, surgery combined with adjuvant chemotherapy remains the standard treatment modality for OSCC [3]. Cisplatin (DDP)-based regimens have become the cornerstone of treatment for patients with advanced-stage disease. However, in clinical practice, DDP frequently causes severe toxicity, and optimal therapeutic efficacy is rarely achieved [4]. The development of chemoresistance represents a major obstacle to the effectiveness of DDP as an anticancer agent. Therefore, the identifica-

https://doi.org/10.62347/FYCN1299

tion of molecular targets to enhance chemosensitivity remains a critical research priority.

Circular RNAs (circRNAs) are a class of endogenous RNAs widely present in cells and possessing diverse biological functions. They are primarily formed through back-splicing, resulting in covalently closed-loop structures without polyadenylation tails [5]. Extensive studies have demonstrated that circRNAs regulate a wide range of physiological and pathological processes, and their abnormal expression has been linked to multiple diseases [6, 7]. Furthermore, circRNA dysregulation plays a critical role in modulating malignant phenotypes of tumor cells [8]. The involvement of circRNAs in OSCC has been extensively investigated. For instance, Shi et al. [9] identified upregulation of Circ_0004771 in OSCC tissues, which exhibited significant predictive value for tumor occurrence, prognosis, recurrence, and patient survival. Qi et al. [10] reported that Circ_0004674 expression was elevated in OSCC, and its knockdown inhibited the progression of OSCC cells in vitro. Gu et al. [11] revealed that CircGDI2 binds to fat mass and obesity associated (FTO) protein, reducing RNA m6A modification levels and suppressing the growth and migration of OSCC cells. Additionally, hsa_circRNA_101036 exacerbates hypoxia-induced endoplasmic reticulum (ER) stress in OSCC via the miR-21-3p/transmembrane and tetratricopeptide repeat containing 1 (TMTC1) axis [12], while circFNDC3B has been shown to alleviate ferroptosis and promote disease progression in OSCC cells by regulating the miR-520d-5p/solute carrier family 7 member 11 (SLC7A11) axis [13].

Other studies have demonstrated that dysregulated circRNAs are closely associated with chemoresistance in tumor cells. Geng et al. [14] confirmed that circHIF1A promotes HIF1α-mediated alterations in glucose metabolism, thereby inducing cetuximab resistance in colorectal cancer. Wang et al. [15] revealed that the knockdown of Circ_0010235 attenuates DPP resistance and tumor growth in lung cancer through the miR-379-5p/E2F transcription factor 7 (E2F7). Meng et al. [16] identified that the CircPTK2/poly(A) binding protein cytoplasmic 1 (PABPC1)/SET domain bifurcated histone lysine methyltransferase 1 (SETDB1) axis facilitates gemcitabine resistance in bladder cancer. Although circFNDC3B has been implicated in the progression of OSCC, no studies to date have investigated its association with chemotherapy resistance in this malignancy, and the underlying mechanisms remain unclear. Therefore, in the present study, we aimed to investigate the regulatory effects of circFNDC3B on DDP resistance in OSCC and to elucidate the potential molecular mechanisms, with the goal of providing a theoretical foundation for overcoming chemotherapy resistance in OSCC.

Materials and methods

Patients and sample collection

This study retrospectively enrolled 68 patients with pathologically confirmed advanced OSCC from the biobank of the Fourth Hospital of Hebei Medical University, diagnosed between December 2021 and December 2023. All patients received first-line cisplatin (DDP)-based chemotherapy regimens (DDP 75-100 mg/m^2 every 3 weeks, or 25-40 mg/m^2 weekly). After 2-3 cycles of DDP-based chemotherapy, therapeutic response was evaluated according to RECIST version 1.1. Eight patients with stable disease (SD) were excluded at this stage to ensure clear discrimination between sensitive and resistant groups, leaving an eligible population of 60 patients for further analysis. The study protocol was approved by the Medical Ethics Committee of the Fourth Hospital of Hebei Medical University (No.2025KY038) in accordance with the Declaration of Helsinki.

Criteria for DDP sensitivity and resistance evaluation

Therapeutic responses were evaluated after 2-3 cycles of DDP-based chemotherapy according to the Response Evaluation Criteria in Solid Tumors (RECIST) version 1.1 [17]. Patients were classified into two groups based on their best overall response:

DDP-sensitive group: Patients achieving complete response (CR) or partial response (PR), defined as a ≥30% decrease in the sum of the longest diameters of target lesions, with no new lesions appearing.

DDP-resistant group: Patients with progressive disease (PD), defined as a ≥20% increase in the

sum of the longest diameters of target lesions or the appearance of new lesions.

Thus, patients achieving complete response (CR) or partial response (PR) were assigned to the DDP-sensitive group, while those with progressive disease (PD) were assigned to the DDP-resistant group.

Inclusion and exclusion criteria

The inclusion criteria were as follows: (1) Age ≥18 years; (2) Histopathologically confirmed OSCC; (3) Received first-line DDP-based chemotherapy; (4) Had at least one measurable lesion according to RECIST 1.1; (5) Complete clinical and follow-up data available; (6) Eastern Cooperative Oncology Group (ECOG) performance status of 0-2.

The exclusion criteria were as follows: (1) Received prior chemotherapy or radiotherapy for OSCC; (2) Coexisting malignant tumors; (3) Severe organ dysfunction (cardiac, hepatic, or renal insufficiency); (4) Pregnant or lactating women; (5) Incomplete clinical data or loss to follow-up.

Based on the above criteria, 60 patients were finally enrolled, including 30 in the DDP-sensitive group and 30 in the DDP-resistant group. Tumor tissue samples were collected during initial biopsy or surgical resection before chemotherapy initiation and immediately frozen in liquid nitrogen until use. Written informed consent was obtained from all patients prior to enrollment.

Animals

Six-week-old male BALB/c nude mice weighing 18 to 20 g were purchased from SLAC Laboratory Animal Co., Ltd. (Shanghai, China). All experimental mice were housed in a specific pathogen-free (SPF) laboratory environment, with strictly controlled ambient temperature at 22±2°C, relative humidity maintained at approximately 60%, and a standard 12 h light/12 h dark circulation cycle. Sterilized standard feed and drinking water were provided ad libitum throughout the experimental period. All animal procedures were approved by the Institutional Animal Care and Use Committee of the Fourth Hospital of Hebei Medical University.

Bioinformatics analysis

The StarBase (ENCORI) database (http://starbase.sysu.edu.cn/) was employed to predict the interaction between circFNDC3B and miR-206, as well as the putative binding sites of miR-206 on the 3'-untranslated region (3'-UTR) of Annexin A2 (ANXA2).

Cell transfection

OSCC cell lines, obtained from the China Cell Research Institute Center (Shanghai, China), were cultured in Dulbecco's Modified Eagle Medium (DMEM) supplemented with 10% fetal bovine serum (FBS). The incubation condition was set at 37°C with 5% CO_2. To maintain drug resistance, CAL-27/DDP and SCC-9/DDP cells were cultured in the same medium supplemented with 5 μM DDP, according to the previously described method [18]. For all transfection experiments and subsequent functional assays, maintenance DDP was withdrawn 24 hours prior to transfection, and cells were cultured in DDP-free medium throughout transfection and the following 48-hour incubation period to eliminate drug interference on viability and apoptosis readouts. For transfection, CAL-27/DDP and SCC-9/DDP cells were transfected using Lipofectamine™ 2000 when the confluence reached approximately 80%. Specifically, for each well, 2 μg of plasmid DNA or 20 nM of siRNA/miRNA mimic/inhibitor was diluted in 250 μL of Opti-MEM (Gibco), while 5 μL of Lipofectamine 2000 was diluted in another 250 μL of Opti-MEM. After a 5-min incubation at room temperature, the two solutions were gently mixed and incubated for an additional 20 min to allow complex formation. The complexes were then added dropwise to each well. The medium was replaced with fresh complete medium 6 hours post-transfection, and cells were harvested for further analyses 48 hours later. The experimental design included the following groups: si-negative control (NC, 5'-GAACCACCTATACCCTGGA-3') group, si-circFNDC3B (5'-TTCAGTGCATTCAAGGAAG-3') group, vector group, pcDNA-circFNDC3B group, si-circFNDC3B+NC inhibitor group, si-circFNDC3B+miR-206 inhibitor (5'-CCACACACUUCCUUACAUUCCA-3') group, NC mimic (5'-CAGUACUUUUGUGUAGUACAA-3') group, miR-206 mimic (5'-UGGAAUGUAAGGAAGUGUGUGG-3')

group, miR-206 mimic+Vector group, and miR-206 mimic+pcDNA-ANXA2 group.

qRT-PCR

Total cellular RNA was extracted from CAL-27/DDP and SCC-9/DDP cells using TRIzol reagent. According to the kit's instructions, the extracted RNA was then reverse-transcribed into cDNA. The expression levels of circFNDC3B and miR-206 were measured via SYBR Green real-time quantitative PCR (Wuhan Xavier Biotechnology Co., Ltd., Wuhan). GAPDH and U6 were used as the endogenous controls for data normalization. Relative transcription levels of the target genes were calculated using the $2^{-\Delta\Delta Ct}$ method. The primer sequences were as follows: for circFNDC3B, forward 5'-TCAGTGCATTCAAGGAAGCC-3' and reverse 5'-CCATCCTCTGCTCTTATTGTGAA-3'; for GAPDH, forward 5'-GGAGCGAGATCCCTCCAAAAT-3' and reverse 5'-GGCTGTTGTCATACTTCTCATGG-3'; for miR-206, forward 5'-AGGCCACATGCTTCTTTATATCCC-3' and reverse 5'-CGAAACCACACACTTCCTTACATT-3'; and for U6, forward 5'-GCTTCGGCAGCACATATAC-3' and reverse 5'-ATTTGCGTGTCATCCTTGC-3'.

Cell counting kit-8 (CCK-8) assay

Cells in the logarithmic growth phase were harvested and resuspended to obtain a uniform single-cell suspension. A volume of 100 μL cell suspension was seeded into each well of 96-well plates. The cells were then incubated in 5% CO_2 at 37°C until they fully recovered from the plating process. Subsequently, the cells were treated with drug according to group assignments and cultured continuously for 48 h. Afterwards, 10 μL CCK-8 working solution was added to each well, followed by 2 h incubation under the same culture conditions. Cell viability was determined by measuring the absorbance at 450 nm using a microplate reader.

Flow cytometry

Cell apoptosis was assessed using Annexin V-FITC/Propidium Iodide (PI) double staining kits (Hangzhou Lianike Biotechnology Co., Ltd., China). Cells were digested, harvested and resuspended in 1× binding buffer at a density of 5×10^5 cells. Then, 5 μL of Annexin V-FITC and 10 μL of PI staining solution were added to the cell suspension, with gentle mixing performed. The reaction was conducted in the dark for 10 minutes. The apoptosis rate was assessed with a flow cytometer.

Western blot

Radioimmunoprecipitation assay (RIPA) buffer was utilized to extract proteins from the cells or tissues, and bicinchoninic acid (BCA) quantification was conducted. Protein samples were separated by sodium dodecyl sulfate-polyacrylamide gel electrophoresis (SDS-PAGE) electrophoresis and transferred onto polyvinylidene fluoride (PVDF) membranes. The membranes were blocked with skimmed milk powder for 1 hour at room temperature, then incubated with primary rabbit anti-ANXA2 antibody (Abcam, 1:1000, USA) overnight at 4°C. Next, the secondary antibody (goat anti-rabbit IgG, Abcam, 1:5000, USA) was applied and incubated for 2 h. The chemiluminescence substrate was then used to detect the protein bands, and Image J software was utilized to analyze the grayscale intensity.

Dual luciferase reporter gene assay

Wild-type (circFNDC3B-WT) and mutant-type (circFNDC3B-MUT) luciferase reporter plasmids containing the predicted miR-206 binding sequence of circFNDC3B were constructed and inserted into the pmirGLO dual-luciferase vector. These plasmids were then co-transfected into CAL-27/DDP and SCC-9/DDP cells along with either the NC mimic or the miR-206 mimic. Luciferase activity was measured on a Dual-Luciferase Reporter Assay System (Promega, USA) with a microplate reader (TECAN, Switzerland).

Xenograft tumor assay

The pretreated CAL-27/DDP cells (transfected with si-NC or si-circFNDC3B) were enzymatically dissociated using trypsin, counted, and resuspended in phosphate-buffered saline (PBS). A total of 100 μL cell suspension was subcutaneously injected into the right axillary region of each nude mouse. All model mice received intraperitoneal injection of DDP at a dose of 3 mg/kg once a week, with all operations performed under strict aseptic conditions. Tumor growth was monitored once a week, and the longest and shortest diameters of each

Table 1. Clinicopathological characteristics of OSCC patients

Characteristics	DDP-sensitive group (n=30)	DDP-resistant group (n=30)	*p*-value
Age (years)			
Mean ± SD	58.3 ± 10.2	59.1 ± 9.8	0.742
Median (range)	57 (32-76)	60 (34-78)	0.698
Gender, n (%)			0.815
Male	22 (73.3)	21 (70.0)	
Female	8 (26.7)	9 (30.0)	
TNM stage, n (%)			0.624
I-II	10 (33.3)	12 (40.0)	
III-IV	20 (66.7)	18 (60.0)	
Tumor location, n (%)			0.538
Tongue	15 (50.0)	13 (43.3)	
Gingiva	8 (26.7)	10 (33.3)	
Buccal mucosa	5 (16.7)	4 (13.3)	
Other	2 (6.7)	3 (10.0)	
Differentiation, n (%)			0.791
Well differentiated	9 (30.0)	10 (33.3)	
Moderately differentiated	15 (50.0)	14 (46.7)	
Poorly differentiated	6 (20.0)	6 (20.0)	
ECOG performance status, n (%)			0.673
0	11 (36.7)	12 (40.0)	
1	16 (53.3)	15 (50.0)	
2	3 (10.0)	3 (10.0)	

Data are presented as n (%) or mean ± standard deviation (SD). *P*-values were calculated using chi-square test or Fisher's exact test for categorical variables, and Student's t-test or Mann-Whitney U test for continuous variables. *P*-values indicate the statistical significance of differences between the groups, and P<0.05 was set as statistically significant. TNM, tumor-node-metastasis; ECOG, Eastern Cooperative Oncology Group.

tumor were measured with a caliper to calculate tumor volume. Four weeks after treatment, the mice were euthanized by cervical dislocation, and the tumor tissues were removed and weighed. One part of each tumor sample was used to test circFNDC3B, miR-206, and ANXA2 protein levels. The remaining tissue was fixed in formalin and embedded in paraffin, and immunohistochemistry was carried out to assess Ki67 expression in the subcutaneous tumors from the different groups.

Immunohistochemistry

The sections were deparaffinized in xylene and rehydrated in graded alcohols. Ethylenediaminetetraacetic acid (EDTA) was used for antigen retrieval. Next 5% bovine serum was added for incubation for 20 minutes. Then, anti-Ki67 (Abcam, USA) was added and incubated overnight at 4°C. After thorough washing, horseradish peroxidase (HRP)-conjugated secondary antibody (Abcam, USA) was added, followed by visualization with 3,3'-Diaminobenzidine (DAB) substrate. Following this the tissue was counterstained with hematoxylin for 2 minutes, and the sections were differentiated three times with hydrochloric acid-ethanol solution for 2 seconds each time. Dehydration was carried out using a graded ethanol series, and the sections were cleared with xylene. Finally, the sections were mounted with neutral gum and examined under a light microscope.

Statistical methods

Statistical analysis of the experimental data was performed using SPSS 25.0 and GraphPad Prism 8. To compare differences between the two groups, Student's t-test was employed. For comparisons involving multiple groups, one-way analysis of variance (ANOVA) followed by Tukey's post-hoc test was utilized. In all data, a *p*-value <0.05 was considered statistically significant.

Results

The baseline clinicopathological characteristics of the enrolled OSCC patients are summarized in **Table 1**. No significant differences were observed between the DDP-sensitive and DDP-resistant groups in terms of age, sex, TNM stage, tumor location, differentiation, or ECOG score (all P>0.05), indicating comparability between the two groups.

Knockdown of circFNDC3B could inhibit the resistance of OSCC cells to DDP

circFNDC3B expression was markedly upregulated in tumor tissues from DDP-resistant OSCC patients (**Figure 1A**). Subsequently, qRT-PCR

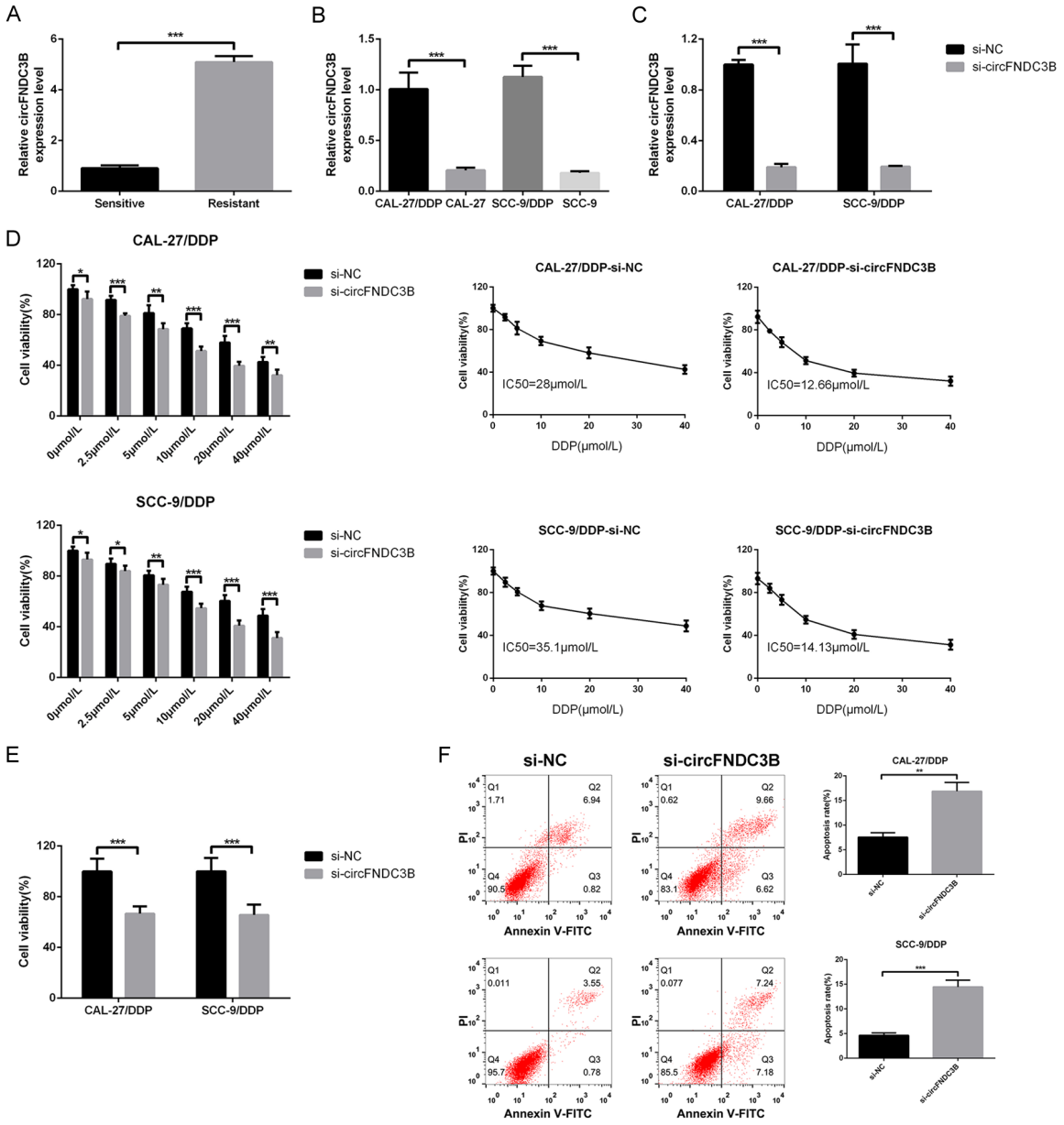


Figure 1. Knockdown of circFNDC3B could inhibit the resistance of OSCC cells to DDP. A. qRT-PCR was used to detect the expression of circFNDC3B in DDP-resistant and DDP-sensitive OSCC tissues. B. qRT-PCR was used to detect the expression of circFNDC3B in OSCC DDP-resistant cell lines CAL-27/DDP and SCC-9/DDP and parental cells CAL-27 and SCC-9. C. qRT-PCR was used to detect the expression level of circFNDC3B in CAL-27/DDP and SCC-9/DDP cells after silencing circFNDC3B. D. CCK-8 assay was used to detect the cell viability and IC_{50} value of DDP in OSCC cells after silencing circFNDC3B at different DDP concentrations. E. CCK-8 assay was used to detect the cell viability of CAL-27/DDP and SCC-9/DDP cells after silencing circFNDC3B. F. Flow cytometry was used to detect the apoptosis of CAL-27/DDP and SCC-9/DDP cells after silencing circFNDC3B. *P<0.05, **P<0.01, ***P<0.001. OSCC: oral squamous cell carcinoma; DDP: Cisplatin; CCK-8: Cell counting kit-8.

analysis demonstrated that circFNDC3B expression was significantly increased in CAL-27/DDP and SCC-9/DDP cells in contrast with CAL-27 and SCC-9 (**Figure 1B**). Next, we transfected si-circFNDC3B into CAL-27/DDP and SCC-9/DDP cells. The resulting expression levels of circFNDC3B were remarkably reduced in contrast with those in the si-NC group, confirming successful transfection (**Figure 1C**). circFNDC3B silencing significantly decreased cell viability and the IC_{50} value of DDP (**Figure 1D**, **1E**). Flow cytometry analysis further demonstrated that

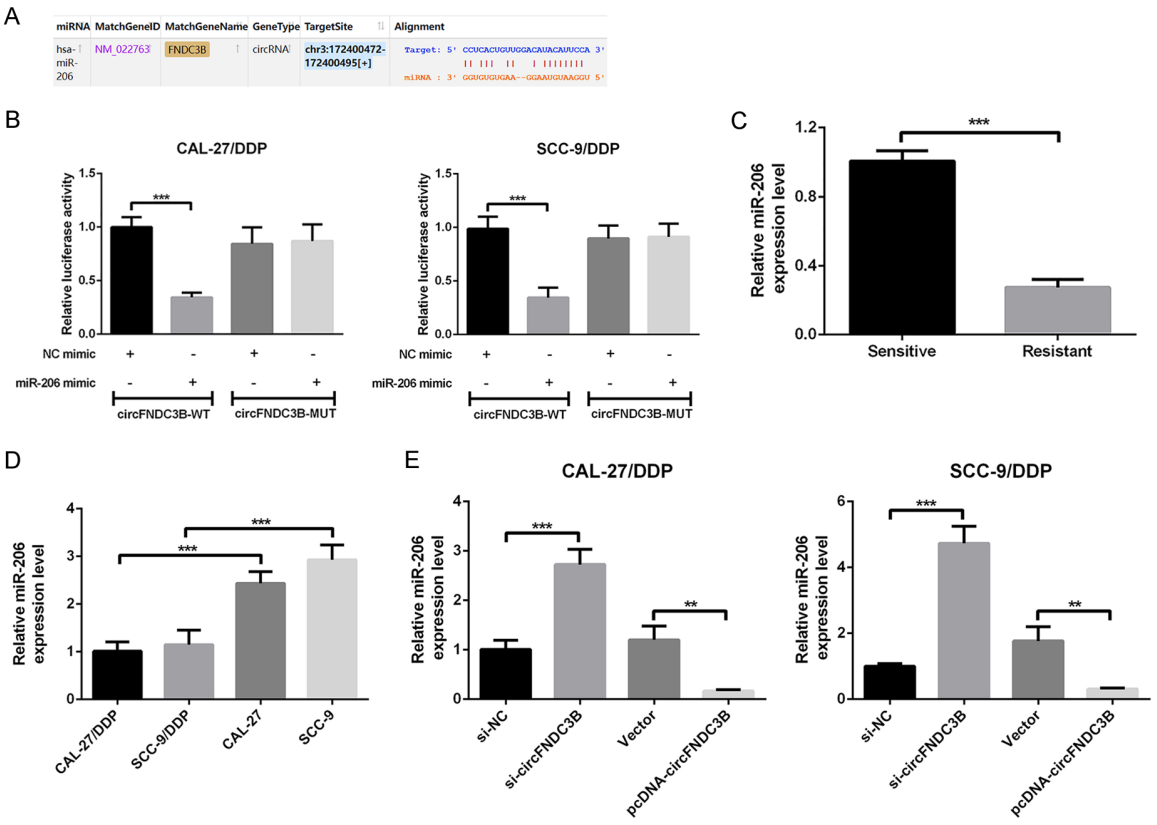


Figure 2. circFNDC3B targeted and regulated the expression of miR-206. A. Bioinformatics software was employed to predict the binding site between circFNDC3B and miR-206. B. A dual-luciferase reporter gene assay was conducted in CAL-27/DDP and SCC-9/DDP cells to confirm the interaction between circFNDC3B and miR-206. C. The expression levels of miR-206 were detected by qRT-PCR in DDP-resistant and DDP-sensitive OSCC patient samples. D. qRT-PCR was used to analyze the expression of miR-206 in DDP-resistant OSCC cell lines (CAL-27/DDP and SCC-9/DDP) as well as their parental cell lines (CAL-27 and SCC-9). E. After silencing or overexpressing circFNDC3B, the expression levels of miR-206 were measured by qRT-PCR in CAL-27/DDP and SCC-9/DDP cells. **P<0.01, ***P<0.001. OSCC: Oral squamous cell carcinoma; DDP: Cisplatin.

circFNDC3B knockdown significantly promoted apoptosis (**Figure 1F**). Collectively, these findings indicate that silencing circFNDC3B effectively diminishes DDP resistance, suppresses cell viability, and induces apoptosis in OSCC cells.

circFNDC3B targeted and regulated the expression of miR-206

The direct interaction between circFNDC3B and miR-206 was predicted using the StarBase database (**Figure 2A**). Dual-luciferase reporter assays demonstrated that co-transfection with miR-206 mimic and circFNDC3B-WT significantly decreased luciferase activity in contrast with the NC mimic group, whereas no significant change was observed for circFNDC3B-mut, confirming specific binding between circFNDC3B and miR-206 (**Figure 2B**). qRT-PCR results revealed that the expression level of miR-206 was markedly decreased in tumor tissues from DDP-resistant OSCC patients in contrast with DDP-sensitive OSCC patients (**Figure 2C**). Additionally, miR-206 expression was downregulated in drug-resistant CAL-27/DDP and SCC-9/DDP cells relative to their parental CAL-27 and SCC-9 cells (**Figure 2D**). Knock down of circFNDC3B led to an increase in miR-206 expression, while overexpression of circFNDC3B resulted in the opposite effect (**Figure 2E**). These findings indicate that circFNDC3B directly targets and negatively regulates miR-206 expression.

circFNDC3B regulated DDP resistance in OSCC cells via targeting miR-206

To further explore the function of circFNDC3B/miR-206 axis in DDP-resistant OSCC cells, cells were transfected with si-NC, si-circFNDC3B, si-circFNDC3B+NC inhibitor, and si-circFNDC3B+

miR-206 inhibitor. Knockdown of circFNDC3B not only upregulated miR-206 expression but also significantly reduced the DDP IC_{50} and cell viability, while substantially increasing the apoptosis rate. Importantly, the inhibitory effects of circFNDC3B knockdown were reversed by co-transfection with the miR-206 inhibitor (**Figure 3A-D**). These data reveal that circFNDC3B knockdown inhibits the malignant progression of DDP-resistant OSCC cells through modulation of miR-206 expression.

miR-206 targeted and regulated the expression of ANXA2

The StarBase (ENCORI) database predicted a direct interaction between miR-206 and ANXA2 (**Figure 4A**). Dual-luciferase reporter assays showed that the miR-206 mimic lowered the luciferase activity of the ANXA2-WT construct compared to the NC mimic, whereas no significant effect was observed on the ANXA2-MUT construct, confirming specific binding between miR-206 and ANXA2 (**Figure 4B**). The protein level of ANXA2 was significantly higher in DDP-resistant OSCC patients than in DDP-sensitive OSCC patients (**Figure 4C**). Furthermore, compared with CAL-27 and SCC-9 cells, the protein expression levels of ANXA2 were markedly elevated in the resistant cell lines (**Figure 4D**). Knockdown of circFNDC3B significantly reduced ANXA2 protein levels, an effect that was effectively reversed by co-transfection with the miR-206 inhibitor (**Figure 4E**). The above results demonstrate that miR-206 directly targets and negatively regulates ANXA2 expression.

miR-206 regulated DDP resistance in OSCC cells through acting on ANXA2

A series of functional assays demonstrated that miR-206 overexpression reduced ANXA2 protein levels, while significantly suppressing the IC_{50} value of DDP and cell viability, and markedly enhancing apoptosis. Conversely, co-transfection with pcDNA-ANXA2 effectively reversed these effects (**Figure 5A-D**). The above results demonstrate that miR-206 upregulation inhibits the progression of DDP-resistant OSCC cells by reducing ANXA2 expression.

Effect of circFNDC3B silencing on the subcutaneous tumor formation of OSCC DDP-resistant cells in nude mice

Knockdown of circFNDC3B significantly reduced xenograft tumor volume and weight (**Figure 6A-C**). Furthermore, circFNDC3B silencing markedly decreased circFNDC3B and ANXA2 expression, while increasing miR-206 level in tumor tissues (**Figure 6D-F**). Immunohistochemical analysis further indicated that Ki67, a proliferation marker, was downregulated in tumor tissues following circFNDC3B knockdown (**Figure 6G**). Collectively, these findings indicate that circFNDC3B suppression effectively inhibits tumor growth in OSCC in vivo, but its effect on cisplatin sensitivity requires further investigation.

Discussion

OSCC is the most prevalent malignant tumor in the head and neck region. The development of OSCC results from multiple factors, stages, and genetic alterations. Despite ongoing improvements in treatment strategies, the prognosis of OSCC patients remains poor, largely due to chemoresistance, a major contributor to unfavorable outcomes [19]. Given that DDP remains the cornerstone of chemotherapy for OSCC, elucidating the mechanisms underlying DDP resistance is of great significance for enhancing therapeutic outcomes.

Accumulating evidence has confirmed that circRNAs are extensively involved in the regulation of gene expression and play critical roles in tumor initiation, progression, and chemoresistance. For instance, Dong et al. [20] confirmed that CircRNA LOC729852 regulates macrophage polarization via the miR-769-5p/Interleukin 10 (IL-10) axis, thereby promoting bladder cancer progression. Fei et al. [21] identified that circ_0008315 modulates the characteristics of gastric cancer stem cells via the miR-3666/CPEB4 axis, thus enhancing DDP resistance and driving malignant progression in gastric cancer. Lei et al. [22] reported that circ_ARHGEF28, as a novel circRNA, promotes DDP resistance in ovarian cancer by inhibiting the Hippo pathway. Recent research has highlighted the association between circFNDC3B and the development of various tumors. Notably, circFNDC3B is upregulated in OSCC and positively correlates with lymph node metastasis. circFNDC3B enhances vascular endothelial growth factor A (VEGFA) transcription and subsequently promotes angiogenesis [23]. However, the function of circFNDC3B in DDP resistance in OSCC remains unclear. Herein, we found that circFNDC3B is highly expressed in

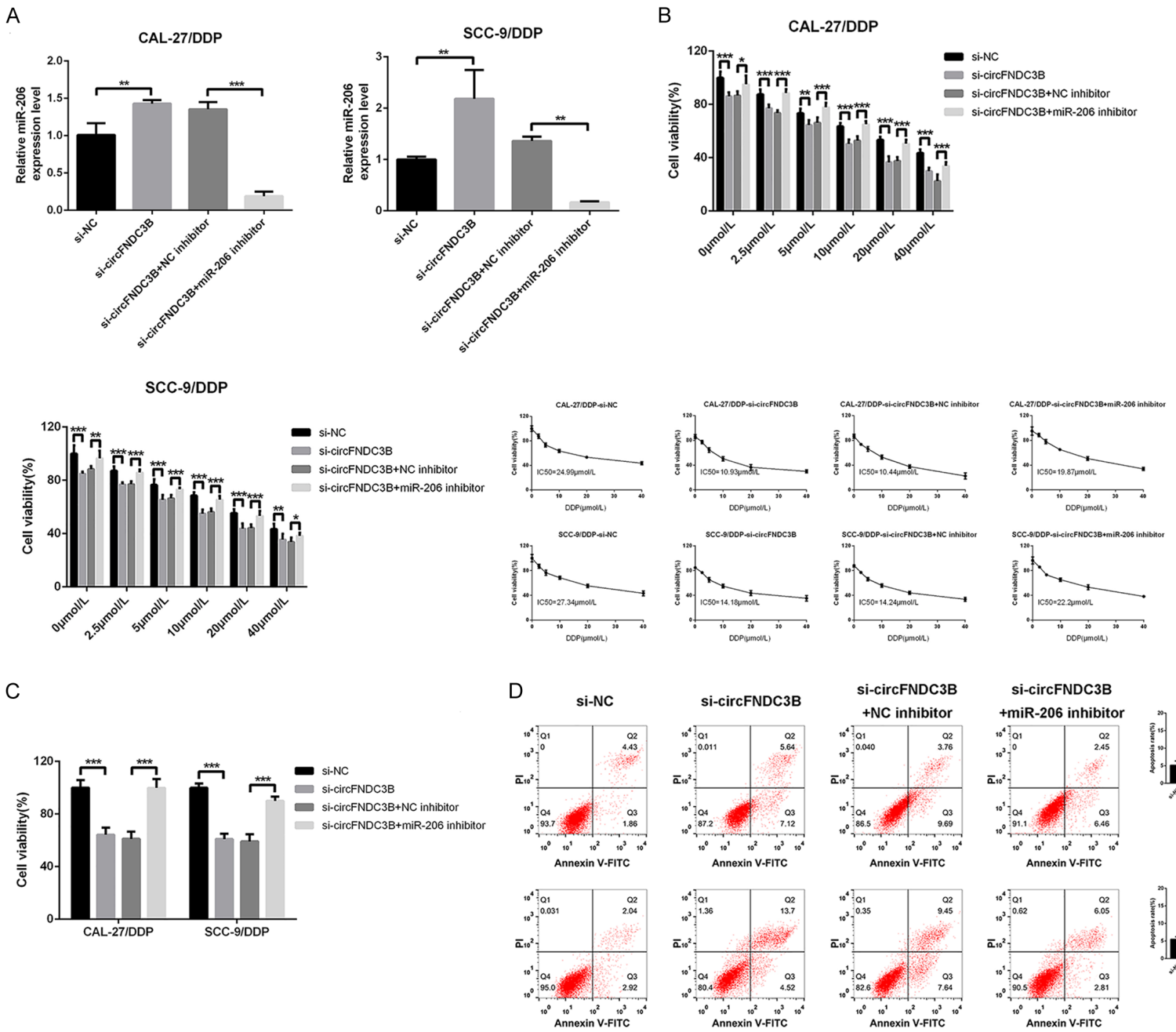

A
CAL-27/DDP
SCC-9/DDP
Relative miR-206 expression level
si-NC
si-circFNDC3B
si-circFNDC3B+NC inhibitor
si-circFNDC3B+miR-206 inhibitor
B
CAL-27/DDP
SCC-9/DDP
Cell viability(%)
0μmol/L
2.5μmol/L
5μmol/L
10μmol/L
20μmol/L
40μmol/L
CAL-27/DDP-si-NC
CAL-27/DDP-si-circFNDC3B
CAL-27/DDP-si-circFNDC3B+NC inhibitor
CAL-27/DDP-si-circFNDC3B+miR-206 inhibitor
SCC-9/DDP-si-NC
SCC-9/DDP-si-circFNDC3B
SCC-9/DDP-si-circFNDC3B+NC inhibitor
SCC-9/DDP-si-circFNDC3B+miR-206 inhibitor
IC50=24.99μmol/L
IC50=10.93μmol/L
IC50=10.44μmol/L
IC50=19.87μmol/L
IC50=27.34μmol/L
IC50=14.18μmol/L
IC50=14.24μmol/L
IC50=22.2μmol/L
DDP(μmol/L)
C
Cell viability(%)
CAL-27/DDP
SCC-9/DDP
D
si-NC
si-circFNDC3B
si-circFNDC3B +NC inhibitor
si-circFNDC3B +miR-206 inhibitor
PI
Annexin V-FITC
Q1
Q2
Q3
Q4
4.43
5.64
3.76
2.45
93.7
87.2
86.5
91.1
1.86
7.12
9.69
6.46
2.04
13.7
9.45
6.05
95.0
80.4
82.6
90.5
2.92
4.52
7.64
2.81
Apoptosis rate(%)

Figure 3. circFNDC3B regulated DDP resistance in OSCC cells by targeting miR-206. A. The expression levels of miR-206 in CAL-27/DDP and SCC-9/DDP cells were measured using qRT-PCR across all groups. B. CCK-8 assays were conducted to evaluate the viability of OSCC drug-resistant cells under various concentrations of DDP, as well as to determine the IC_{50} values for DDP. C. CCK-8 assays were further employed to assess the cell viability of CAL-27/DDP and SCC-9/DDP cells. D. Flow cytometry was used to analyze apoptosis in CAL-27/DDP and SCC-9/DDP cells. *P<0.05, **P<0.01, ***P<0.001. OSCC: oral squamous cell carcinoma; DDP: Cisplatin; CCK-8: Cell counting kit-8.

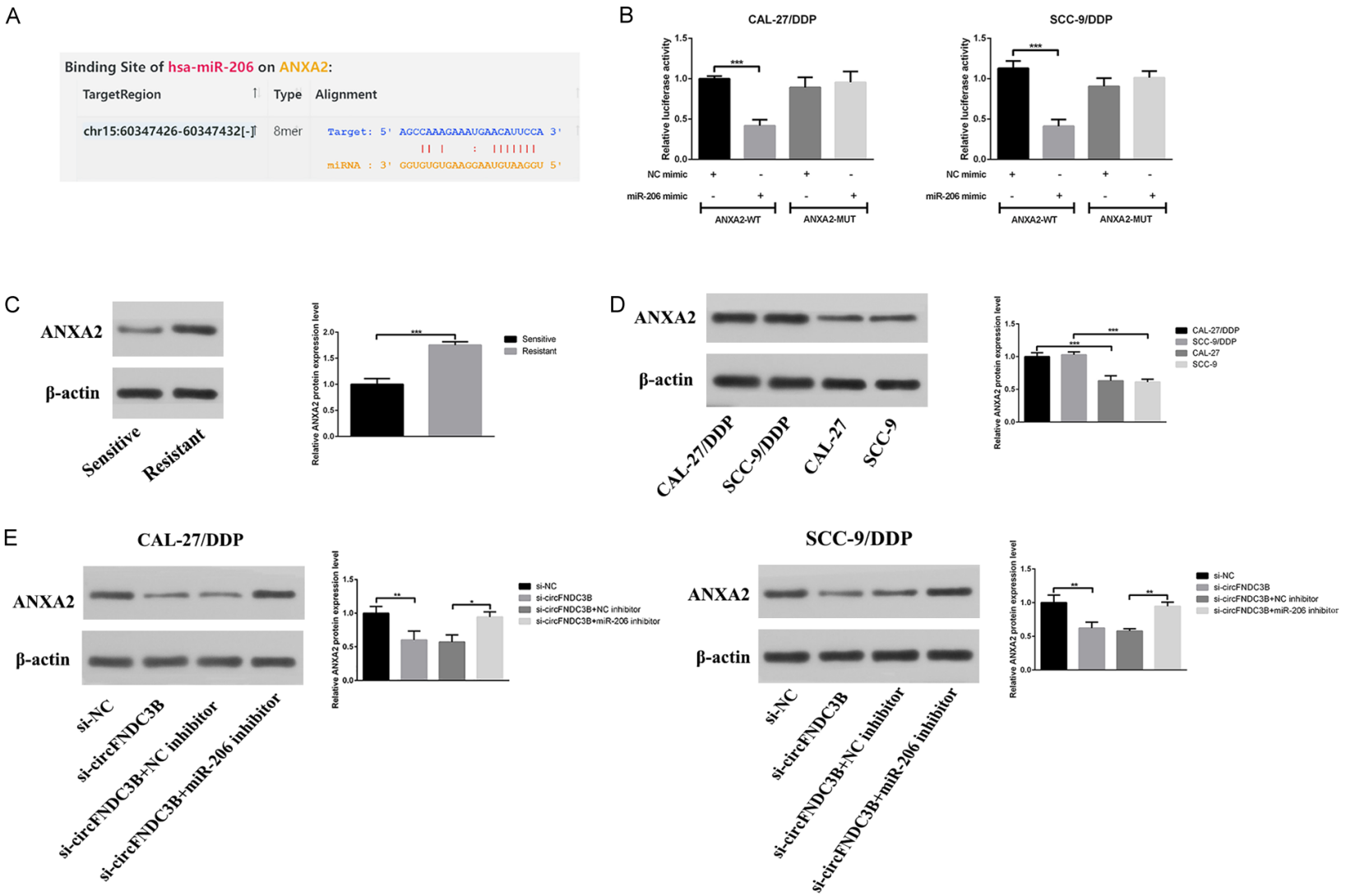
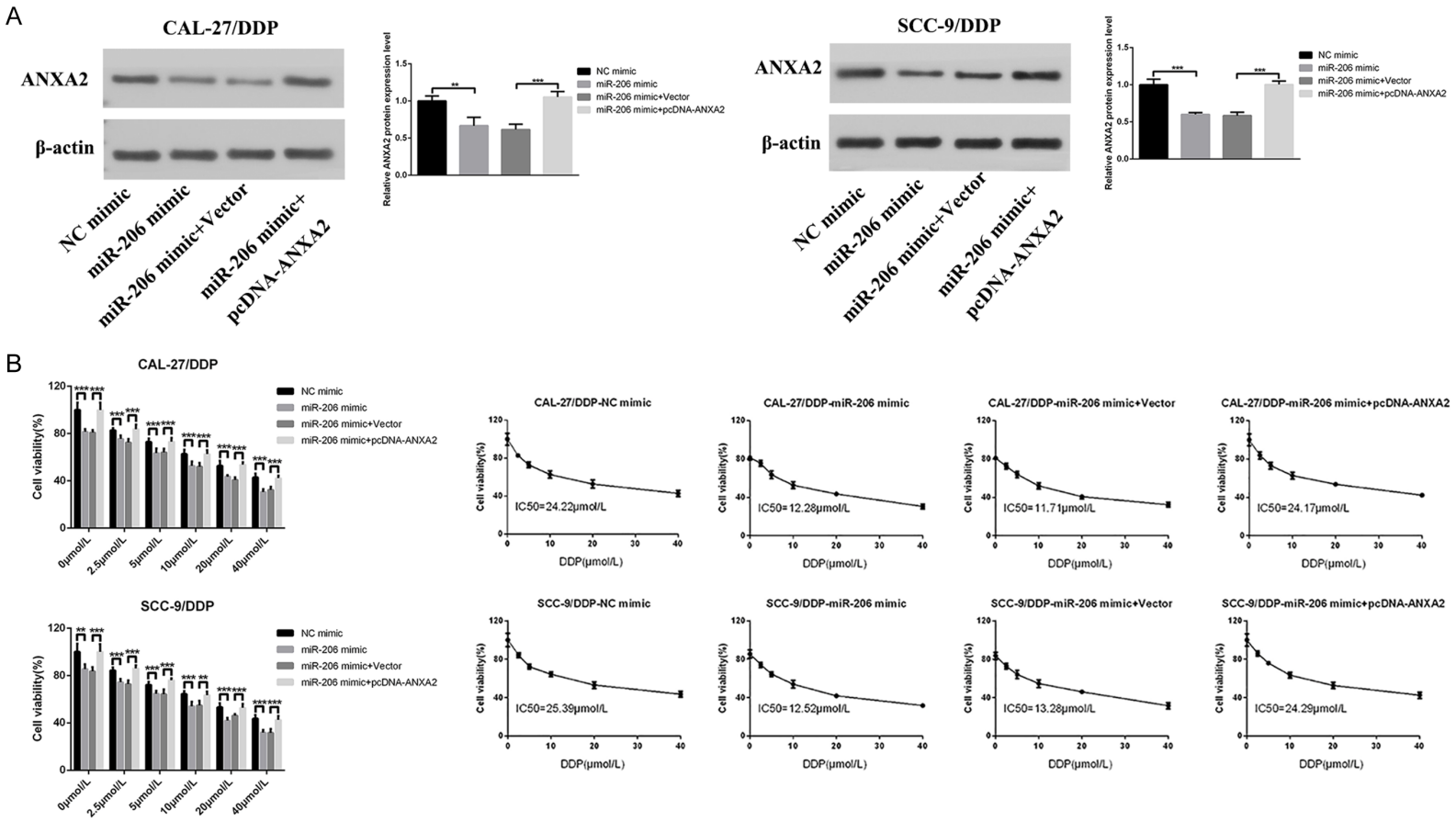


Figure 4. miR-206 targeted and regulated the expression of ANXA2. A. Bioinformatics software was employed to predict the binding sites of miR-206 and ANXA2. B. Dual-luciferase reporter assays were conducted to verify the targeting relationship between miR-206 and ANXA2. C. Western blot analysis was performed to detect the expression of ANXA2 protein in DDP-resistant and DDP-sensitive OSCC patients. D. Western blot analysis was used to evaluate the expression of ANXA2 protein in DDP-resistant OSCC cell lines and their parental cells. E. Western blot analysis was carried out to determine the ANXA2 protein expression levels in CAL-27/DDP and SCC-9/DDP cells. *P<0.05, **P<0.01, ***P<0.001. OSCC: oral squamous cell carcinoma; ANXA2: Annexin A2; DDP: Cisplatin.



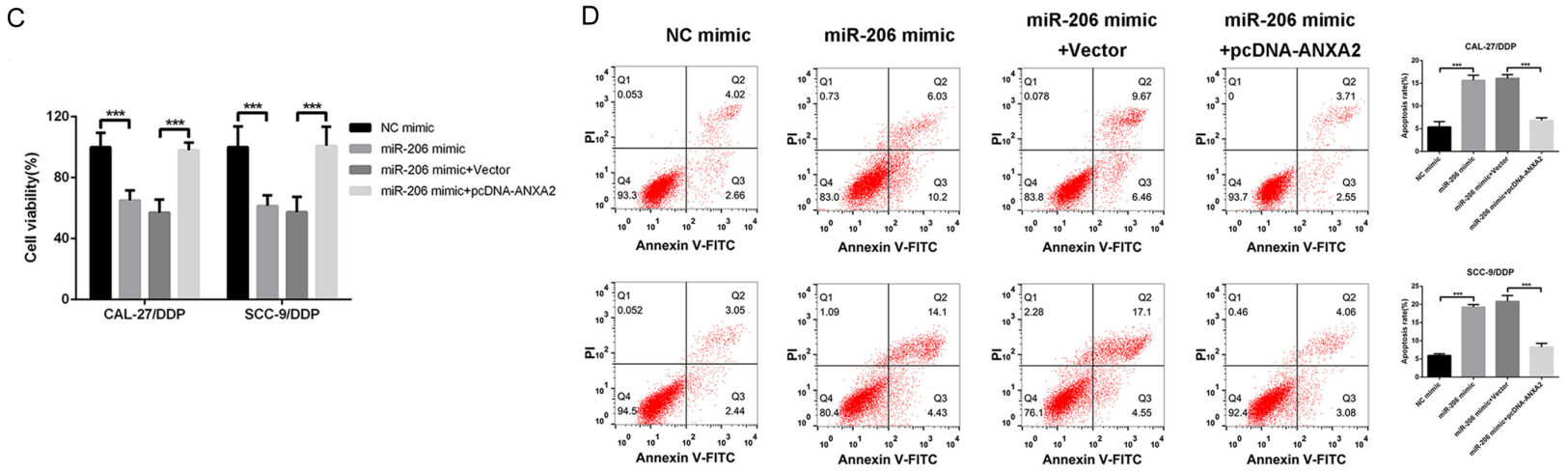


Figure 5. miR-206 regulated DDP resistance in OSCC cells by targeting ANXA2. A. Western blot analysis was employed to detect the expression levels of ANXA2 protein in CAL-27/DDP and SCC-9/DDP cells. B. The CCK-8 assay was conducted under various concentrations of DDP to evaluate the viability of OSCC cells and determine the IC_{50} value for resistant cells. C. The CCK-8 assay was further utilized to assess the cell viability of CAL-27/DDP and SCC-9/DDP cells. D. Flow cytometry was performed to analyze apoptosis in CAL-27/DDP and SCC-9/DDP cells. **P<0.01, ***P<0.001. OSCC: oral squamous cell carcinoma; ANXA2: Annexin A2; DDP: Cisplatin; CCK-8: Cell counting kit-8.

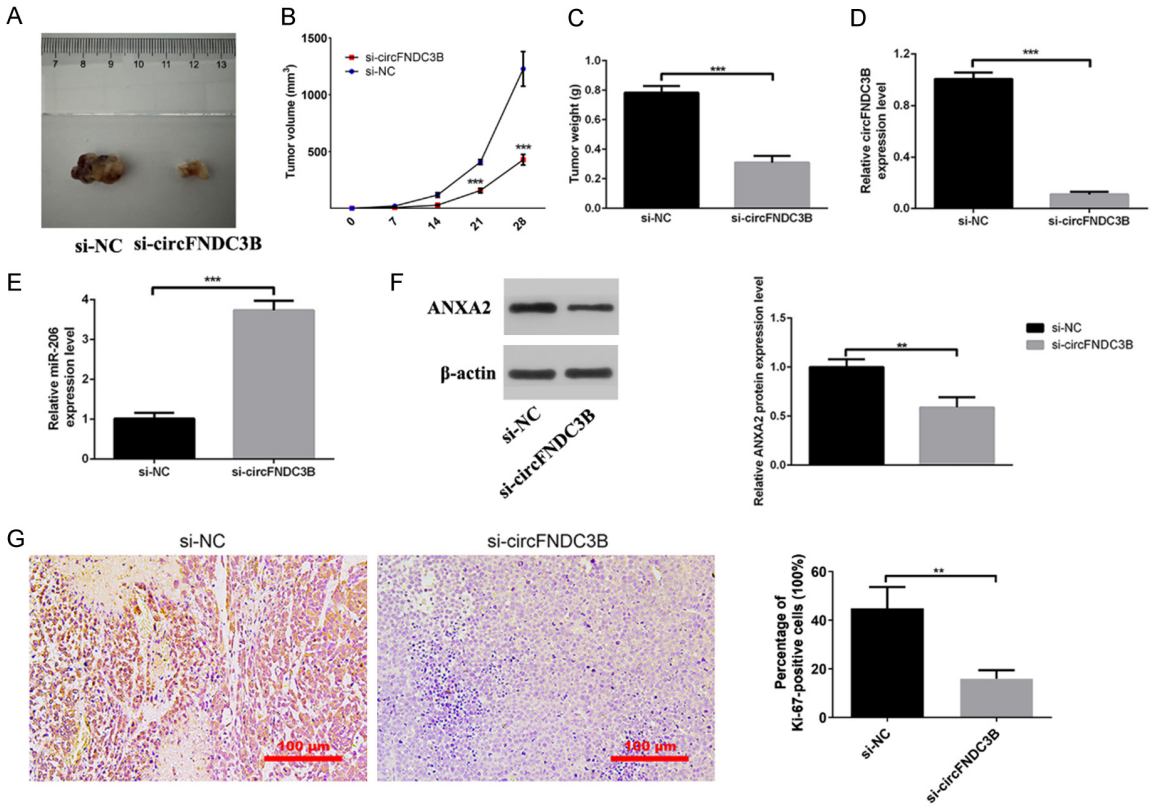


Figure 6. Effect of circFNDC3B silencing on the subcutaneous tumorigenesis of OSCC DDP-resistant cells in nude mice. A. Tumor volumes in nude mice at 28 days. B. Subcutaneous tumor growth curve. C. Analysis of subcutaneous tumor weight in each group of nude mice. D. qRT-PCR detection of circFNDC3B expression in subcutaneous tumors of nude mice. E. qRT-PCR detection of miR-206 expression in subcutaneous tumors of nude mice. F. Western blot analysis of ANXA2 protein expression in subcutaneous tumors of nude mice. G. Immunohistochemical analysis of Ki67 expression in subcutaneous tumor tissues of nude mice. **P<0.01, ***P<0.001. OSCC: oral squamous cell carcinoma; DDP: Cisplatin; ANXA2: Annexin A2.

DDP-resistant cells, and its knockdown significantly enhances the sensitivity of DDP-resistant cell lines to DDP, suggesting that circFNDC3B has association with DDP resistance in OSCC.

miRNAs are key regulators involved in diverse human physiological and pathological processes [24]. In recent years, a growing number of studies have shown that circRNAs participate in various biological events. For example, circBIRC6 promotes the progression of prostate cancer by targeting miR-574-5p [25], while circZFR enhances the growth ability and metastasis of colorectal cancer cells by binding to miR-3127-5p [26]. Interestingly, circFNDC3B has also been reported to interact with miRNAs and contribute to cancer development. One study showed that circFNDC3B drives esophageal squamous cell carcinoma progression via the miR-370-3p/miR-136-5p axis [27], whereas another demonstrated that it directly binds to miR-937-5p to suppress colorectal cancer progression [28]. To elucidate the mechanism by which circFNDC3B modulates drug resistance in OSCC, we performed a circRNA-miRNA interaction analysis. The results demonstrated that circFNDC3B can directly bind to miR-206 and negatively regulate its expression, suggesting that circFNDC3B may function as a molecular sponge for miR-206, thereby modulating OSCC chemoresistance. It has been previously shown that miR-206 acts as a tumor suppressor in colorectal cancer, breast cancer, and OSCC [29-31]. In rescue experiments, we combined circFNDC3B knockdown with miR-206 inhibition in resistant cancer cells, and found that miR-206 inhibition effectively reversed the increased DDP sensitivity induced by circFNDC3B knockdown. Collectively, these results indicate that circFNDC3B enhances drug resis-

tance in OSCC cells by targeting miR-206. Together, our findings provide a mechanistic explanation for circFNDC3B-mediated chemoresistance and offer a theoretical basis for therapeutic targeting of the circFNDC3B/miR-206 axis.

To demonstrate the function of miR-206 in OSCC chemoresistance, we performed experiments to predict and validate miRNA target genes. Our findings illustrated that ANXA2 is a direct target of miR-206. ANXA2, a calcium-dependent phospholipid-binding protein, contributes to various cellular biological processes, including proliferation, apoptosis, and drug resistance. Previous research has shown that ANXA2 is overexpressed in various cancers and strongly linked to drug resistance. For instance, ANXA2 promotes esophageal cancer progression by regulating the Akt/mTOR axis [32], and its high expression in esophageal cancer tissues contributes to tumor development through modulation of extracellular signal-regulated kinase (ERK) phosphorylation [33]. Additionally, knockdown of RecQ Like Helicase 4 (RECQL4) reduces the sensitivity of cervical cancer cells to DDP by modulating ANXA2 expression [34]. Herein, miR-206 upregulation significantly inhibits ANXA2 expression, thereby reducing drug resistance in OSCC cells. Taken together, these findings indicate that miR-206 enhances the sensitivity of OSCC cells to DDP by regulating the expression of ANXA2. In summary, our study elucidates a mechanistic axis through which miR-206 mediates drug resistance in OSCC and provides a theoretical basis for targeting the miR-206/ANXA2 axis in future therapy.

For the first time, we have identified the interaction between circFNDC3B, miR-206, and ANXA2 in OSCC drug resistance. This finding offers a theoretical basis for designing new therapies. Admittedly, there are still some weaknesses that need to be considered. First, we did not perform gain-of-function experiments by overexpressing circFNDC3B in parental sensitive cells. Second, we did not conduct in vivo rescue experiments targeting the miR-206/ANXA2 axis in the xenograft model. Third, the lack of a PBS control group in the xenograft model precludes us from distinguishing the intrinsic antitumor effect of circFNDC3B knockdown from its impact on cisplatin sensitivity. Fourth, the CCK-8 assays were performed at single time points, which reflect cell viability rather than genuine proliferation rates. Fifth, the effects of miR-206 alone showed context-dependent heterogeneity, and the observed phenotypes were not always consistent across different cell backgrounds. Sixth, we did not carry out clinical trials or systematic drug screening to validate circFNDC3B as a therapeutic target. Taken together, these limitations indicate that our conclusions should be interpreted with caution and warrant further investigation.

In summary, our study demonstrates that circFNDC3B is highly upregulated in DDP-resistant OSCC, and its knockdown attenuates DDP resistance in OSCC cells via the miR-206/ANXA2 axis, concomitantly suppressing cell viability and promoting apoptosis in DDP-resistant OSCC cells. These findings provide novel insights into the drug resistance mechanisms of OSCC and offer innovative strategies for its treatment. Furthermore, this study is the first to identify circFNDC3B as a central hub within the ceRNA network driving the molecular pathology of chemoresistance in OSCC. It also provides a new molecular marker and theoretical foundation for developing strategies to reverse drug resistance based on RNA-targeted therapy.

Acknowledgements

This study was supported by the Medical Science Research Project of Hebei (grant no. 20240101).

Disclosure of conflict of interest

None.

Address correspondence to: Kunshan Li, Department of Stomatology, The Fourth Hospital of Hebei Medical University, No. 12 Health Road, Shijiazhuang 050000, Hebei, China. Tel: +86-0311-86095436; E-mail: shanshan5679@163.com

References

[1] Radaic A, Kamarajan P, Cho A, Wang S, Hung GC, Najarzadegan F, Wong DT, Ton-That H, Wang CY and Kapila YL. Biological biomarkers of oral cancer. Periodontol 2000 2024; 96: 250-280.

[2] Acharya S, Hegde U, Acharya AB and Nitin P. Dysbiosis linking periodontal disease and oral squamous cell carcinoma-A brief narrative review. Heliyon 2024; 10: e32259.

[3] Jing F, Zhu L, Zhang J, Zhou X, Bai J, Li X, Zhang H and Li T. Multi-omics reveals lactylation-driven regulatory mechanisms promoting tumor progression in oral squamous cell carcinoma. Genome Biol 2024; 25: 272.
[4] Fang K, Sun M, Leng Z, Chu Y, Zhao Z, Li Z, Zhang Y, Xu A, Zhang Z, Zhang L, Chen T and Xu M. Targeting IGF1R signaling enhances the sensitivity of cisplatin by inhibiting proline and arginine metabolism in oesophageal squamous cell carcinoma under hypoxia. J Exp Clin Cancer Res 2023; 42: 73.
[5] Kristensen LS, Jakobsen T, Hager H and Kjems J. The emerging roles of circRNAs in cancer and oncology. Nat Rev Clin Oncol 2022; 19: 188-206.
[6] Sun H, Xie Y, Wu X, Hu W, Chen X, Wu K, Wang H, Zhao S, Shi Q, Wang X, Cui B, Wu W, Fan R, Rao J, Wang R, Wang Y, Zhong Y, Yu H, Zhou BS, Shen S and Liu Y. circRNAs as prognostic markers in pediatric acute myeloid leukemia. Cancer Lett 2024; 591: 216880.
[7] Xu F, Xiao Q, Du WW, Wang S and Yang BB. CircRNA: functions, applications and prospects. Biomolecules 2024; 14; 1503.
[8] Conn VM, Chinnaiyan AM and Conn SJ. Circular RNA in cancer. Nat Rev Cancer 2024; 24: 597-613.
[9] Shi R and Zhang L. Circ_0004771 regulates malignant biological behaviors and has clinical significance in oral squamous cell carcinoma. J Oral Pathol Med 2024; 53: 502-510.
[10] Qi C, Zhang L and Wang W. The novel circ_0004674/miR-139-5p/ZBTB2 regulatory cascade inhibits the development of oral squamous cell carcinoma. Head Neck 2024; 46: 1671-1682.
[11] Gu Y, Sheng L, Wei X, Chen Y, Lin Y, Li Z, Li X, Yang H, Wang Y, Yang H and Shen Y. Upregulation of circGDI2 inhibits tumorigenesis by stabilizing the expression of RNA m6A demethylase FTO in oral squamous cell carcinoma. Noncoding RNA Res 2024; 10: 140-152.
[12] Deng W, Fu J, Lin S, Wen Q, Fu L and Chen X. Hsa_circRNA_101036 aggravates hypoxic-induced endoplasmic reticulum stress via the miR-21-3p/TMTC1 axis in oral squamous cell carcinoma. Heliyon 2024; 10: e32969.
[13] Yang J, Cao XH, Luan KF and Huang YD. Circular RNA FNDC3B protects oral squamous cell carcinoma cells from ferroptosis and contributes to the malignant progression by regulating miR-520d-5p/SLC7A11 axis. Front Oncol 2021; 11: 672724.
[14] Geng Y, Zheng X, Zhang D, Wei S, Feng J, Wang W, Zhang L, Wu C and Hu W. CircHIF1A induces cetuximab resistance in colorectal cancer by promoting HIF1α-mediated glycometabolism alteration. Biol Direct 2024; 19: 36.
[15] Wang L, Wang D, Xu Z, Qiu Y, Chen G and Tan F. Circ_0010235 confers cisplatin resistance in lung cancer by upregulating E2F7 through absorbing miR-379-5p. Thorac Cancer 2023; 14: 1946-1957.
[16] Meng X, Xiao W, Sun J, Li W, Yuan H, Yu T, Zhang X and Dong W. CircPTK2/PABPC1/SETDB1 axis promotes EMT-mediated tumor metastasis and gemcitabine resistance in bladder cancer. Cancer Lett 2023; 554: 216023.
[17] Eisenhauer EA, Therasse P, Bogaerts J, Schwartz LH, Sargent D, Ford R, Dancey J, Arbuck S, Gwyther S, Mooney M, Rubinstein L, Shankar L, Dodd L, Kaplan R, Lacombe D and Verweij J. New response evaluation criteria in solid tumours: revised RECIST guideline (version 1.1). Eur J Cancer 2009; 45: 228-247.
[18] Liu T, Chen G, Sun D, Lei M, Li Y, Zhou C, Li X, Xue W, Wang H, Liu C and Xu J. Exosomes containing miR-21 transfer the characteristic of cisplatin resistance by targeting PTEN and PDCD4 in oral squamous cell carcinoma. Acta Biochim Biophys Sin (Shanghai) 2017; 49: 808-816.
[19] Chen X, Kuang S, He Y, Li H, Yi C, Li Y, Wang C, Chen G, Chen S and Yu D. The differential metabolic response of oral squamous cell carcinoma cells and normal oral epithelial cells to cisplatin exposure. Metabolites 2022; 12: 389.
[20] Dong C, Hui P, Wu Z, Li J and Man X. CircRNA LOC729852 promotes bladder cancer progression by regulating macrophage polarization and recruitment via the miR-769-5p/IL-10 axis. J Cell Mol Med 2024; 28: e18225.
[21] Fei Y, Cao D, Li Y, Wang Z, Dong R, Zhu M, Gao P, Wang X, Cai J and Zuo X. Circ_0008315 promotes tumorigenesis and cisplatin resistance and acts as a nanotherapeutic target in gastric cancer. J Nanobiotechnology 2024; 22: 519.
[22] Lei R, Long Y, Li Q, Xie Q, Ling X, Xie M, Zhou H and Zhang B. Circular RNA circ_ARHGEF28 inhibits MST1/2 dimerization to suppress Hippo pathway to induce cisplatin resistance in ovarian cancer. Cancer Cell Int 2024; 24: 256.
[23] Li X, Wang C, Zhang H, Li Y, Hou D, Liu D, Xu R, Cheng J, Liu L, Fu Y, Ye J and Jiang H. circFNDC3B accelerates vasculature formation and metastasis in oral squamous cell carcinoma. Cancer Res 2023; 83: 1459-1475.
[24] Zabalza A, Pappolla A, Comabella M, Montalban X and Malhotra S. MiRNA-based therapeutic potential in multiple sclerosis. Front Immunol 2024; 15: 1441733.
[25] Zhao B, Yang J, Ran F, Shi Y, Yang L, Duan Y, Shi Z, Li X, Zhang J, Li Z and Wang J. CircBIRC6 affects prostate cancer progression by regulating miR-574-5p and DNAJB1. Cancer Biol Ther 2024; 25: 2399363.

[26] Chen J, Wang H, Xu J, Chen E, Meng Q, Wang J, Xiang H, Zhou W, Shan G, Ju Z and Song Z. CircZFR promotes colorectal cancer progression via stabilizing BCLAF1 and regulating the miR-3127-5p/RTKN2 axis. Sci China Life Sci 2024; 67: 1881-1898.
[27] Song D, Ye Z, Chen F, Zhan L and Sun X. circFNDC3B promotes esophageal squamous cell carcinoma progression by targeting MYO5A via miR-370-3p/miR-136-5p. BMC Cancer 2023; 23: 821.
[28] Zeng W, Liu Y, Li WT, Li Y and Zhu JF. CircFNDC3B sequestrates miR-937-5p to derepress TIMP3 and inhibit colorectal cancer progression. Mol Oncol 2020; 14: 2960-2984.
[29] Hong SA, Lee HJ, Kim OH, Hong M, Kim JW and Kim JY. MicroRNA-206 overexpression is associated with a prominent inflammatory reaction and a favorable colorectal cancer prognosis. Pathol Res Pract 2024; 263: 155573.
[30] Sun D, Li C and Zhang F. MicroRNA-206 suppresses growth and metastasis of breast cancer stem cells via blocking EVI-1-mediated CALR expression. PLoS One 2022; 17: e0274919.
[31] Sekar D, Murthykumar K and Ganapathy D. miR-206 and its mimics: a predictive biomarker and therapeutic molecule in the treatment of oral cancer. Oral Oncol 2022; 128: 105849.
[32] Liu R, Lu Y, Li J, Yao W, Wu J, Chen X, Huang L, Nan D, Zhang Y, Chen W, Wang Y, Jia Y, Tang J, Liang X and Zhang H. Annexin A2 combined with TTK accelerates esophageal cancer progression via the Akt/mTOR signaling pathway. Cell Death Dis 2024; 15: 291.
[33] Li Z, Pan Y, Yao J, Gao Y, Qian Y, Zheng M and Ma S. ANXA2 as a novel substrate of FBXW7 promoting esophageal squamous cell carcinoma via ERK phosphorylation. Biochem Biophys Res Commun 2023; 649: 93-100.
[34] Wang R and Zhang Y. RecQ protein-like 4 drives cisplatin chemosensitivity of cervical cancer cells by modulating annexin A2. Drug Dev Res 2024; 85: e70003.